Lasers in Manufacturing Conference 2015

Processing of High Strength Al-Cu alloy Using 400W Selective Laser Melting – Initial Study

Daniel Koutny[a]*, David Palousek[a], Ondrej Koukal[a], Tomas Zikmund[a], Libor Pantelejev[a], Filip Dokoupil[a]

[a]Brno University of Technology, Faculty of Mechanical Engineering, Institute of Machine and Industrial Design, Brno, Czech Republic
[b]Second affiliation, Address, City and Postcode, Country

Abstract

The proposed paper deals with development of production parameters of high strength Aluminium (Al–Cu–Mg–Fe–Ni) alloy using 400W selective laser melting system. The AW2618 high-strength aluminium alloy is typically used in aerospace and military components, engine pistons, parts of turbochargers due to its ability to work in higher temperature applications. The advantage is the stability of mechanical properties after heating even over 100 °C due to the Ni and Fe content. Due to high energy input of SLM, high heating and cooling rates are induced during the melting/solidification process which gives the ability to process this typically difficult to weld material. First stage of experiments with different values of laser power (LP) and laser scanning speed (LS) were conducted to describe the processing window. Single track scans (STS) with LP 100-400W and LS 200-1400mm/s were processed to find the optimal energy density for Al-Cu alloy. Layer thickness and other parameters stayed unchanged. Continuity and quality of STS were analyzed with non-contact 3D optical profilometer. Second stage of experiments was aimed on processing of multiple layers and homogeneity of the material. The μCT scanning of the samples was used in order to obtain qualitative and quantitative information about the sample porosity. Results show, that with the higher laser power (400W) a relative density higher than 99% can be reached, however with large amount of cracks. To reach the fully dense material free of cracks further experiments are necessary.

* Corresponding author. Tel.: +420-54114-3356
E-mail address: koutny@fme.vutbr.cz

1. Introduction

Selective Laser Melting (SLM) technology has been extensively used (Wohlers 2014) as a manufacturing technology for parts of high complexity mainly in the automotive, aerospace and space industry for topologically optimized components and structured ultra-light constructions (Reinhart and Teufelhart 2011), medicine e.g. production of fixtures and prostheses with porous structure(Fukuda et al. 2011), engineering e.g. special shaped cooling channels and inserts into molds (Wong et al. 2009) and also in research and development of new materials (Petters et al. 2013).

During the SLM process a product is created by gradually applied and melted thin layers of metal powder by laser beam only at the places defined by actual cross-section of part geometry. Compared to conventional production technologies (casting, forging and machining), SLM offers a wide range of benefits, e.g. production with no need for expensive molds, very low material waste and the possibility to create complex geometric shapes. However, the massive implementation of this technology is still limited by available materials.

Aluminum alloys are among the materials that are in the forefront of interest thanks to its good strength to weight ratio and resistance against corrosion. Several issues, associated with the properties of aluminum, have adverse effect on the entire SLM production process. In comparison with other materials, aluminum has high reflectivity, high thermal conductivity and high affinity to oxygen which cause immediate formation of oxides.

Recently Al-Si based alloys, AlSi10Mg and AlSi12 (4xxx series) have been extensively studied (Weingarten et al. 2015; Siddique et al. 2015; E.O. Olakanmi 2013; Eyitayo Olatunde Olakanmi, Dalgarno, and Cochrane 2012; Brandl et al. 2012; Buchbinder et al. 2011; Kempen et al. 2012; Thijs et al. 2013) particularly due to their good weldability compared to high strength aluminium alloys (2xxx and 7xxx series).

The further exploitation of lightweight high performance Al parts directed the research on SLM of Al metal matrix composites. For example, recent research investigated the capability of SLM process for production of in situ reinforcements inside Al matrix (Dadbakhsh et al. 2012; Jerrard et al. 2011; Dadbakhsh & Hao 2014). The finding shows that SLM can activate an in situ reaction in the mixture of pure Al with Fe_2O_3 powders to produce three-dimensional Al matrix composites reinforced with very fine (50 – 100 nm) in situ particles.

Al-Cu and Al-Zn based alloys produced by SLM technology have been investigated as well (Louvis, Fox, and Sutcliffe 2011; Bartkowiak et al. 2011; Ahuja et al. 2014), but the area is still poorly described.

Ahuja et al. dealt with the processing of an EN AW-2618 alloy using SLM technology to achieve high relative density of the material. They used particles with a size from 20 μm to 60 μm. Using 100W laser of 10 μm beam diameter of and 50 μm hatch distance on the SLM 50 from Realizer GmbH they achieved a relative density of up to 99.97%. They also concluded that the supporting structures increase the relative density of the part and the relative density and volumetric energy density are not in a direct correlation.

Development of additive technology for metal parts leads to series production, which requires speed increase. High performance lasers enable to use faster scanning speeds and greater range of appropriate values of hatch distances. Therefore the aim of this initial study is to map the range of SLM process parameters for use with 400W laser and coarser layer thickness.

2. Methods

The main goal of this project is to obtain SLM process parameters for high power laser system and achieve low relative porosity. According previous research (Ahuja et al. 2014) the 99.97% of relative porosity could be attained.

Whole process of development consists of following steps:

1. Metal powder characterization
2. Single track production
3. Thin wall production
4. Cube samples production
5. µCT analyses of cube samples

2.1. Hardware parameters

All samples were produced by SLM 280HL machine equipped with 400W ytterbium fiber laser. Basically the building chamber of the machine is filled up with nitrogen for aluminum parts. Layer thickness was established for al tests on 50 µm. For basic analysis of samples a small reduction building platform was used. Temperature of building platform was adjusted in the control system to 120 °C. However the real actual measured temperature of platform surface was 80 °C.

Table 1. SLM parameters

SLM parameters			
Machine	SLM 280HL (SLM solution)	Atmosphere	Nitrogen
Max. laser power	400W	Overpressure	10–12 mbar
Laser	Ytterbium fibre laser beam	Oxygen level	0.1–0.2%
Operational Beam Focus	82 µm	Reduction built plate temp.	80°C
Beam	Gaussian beam	Built plate temp.	200°C
Layer thickness	50 µm		

3. Results

3.1. Powder characterization

Powder was not additionally sieved and was used in the initial state directly from the vendor. The powder characterization of gas atomized aluminum alloy 2618 (TLS Technik GmbH, 20-63 µm) was performed using several technics. Shape and morphology of particles were analyzed using Zeiss Ultra-Plus 50 Scanning Electron Microscopy (SEM). For chemical analysis the spectrochemical analysis by the spectrometer ICP-OES Thermo iCAP 6500-ICP (Thermo Scientific, USA) was used. Distribution of particle size was measured by Horiba LA-960 laser particle size analyzer (Fig. 1). Particles median size is 51.8 µm, mean size is 53.3 µm, and therefore layer thickness of 50 µm was used during all experiments.

Table 1. Chemical Composition Limits of standard materials

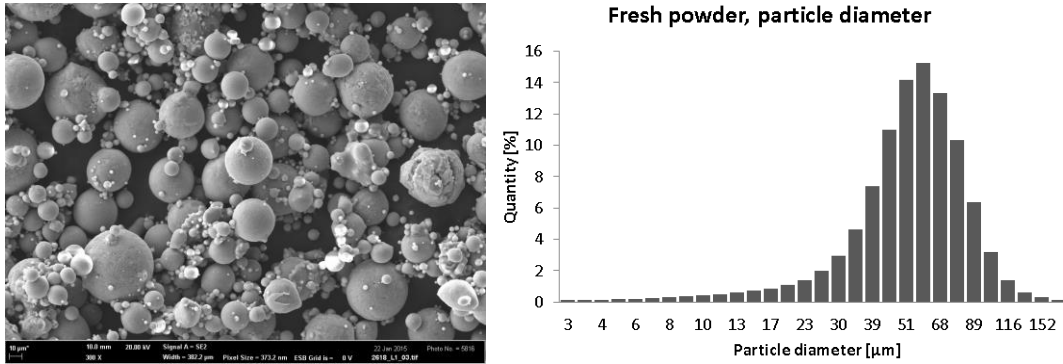| Weight%	Al	Si	Fe	Cu	Mg	Ni	Zn	Ti	Others Total
2618 USA	Rem	0.10-0.25	0.9-1.3	1.9-2.7	1.3-1.8	0.9-1.2	0.10 max	0.04-0.10	0.15 max
2618A EAA	Rem	0.15-0.25	0.9-1.4	1.8-2.7	1.2-1.8	0.8-1.4	0.15 max	0.20 max	0.15 max
SLM powder		**0.149**	**1.00**	**2.66**	**1.39**	**1.22**		**0.20**	

Fig. 1: Powder characterization: SEM image (left) and particle size distribution of alloy 2618 (right)

In addition, cumulative percentage of particle size was evaluated. Particle size up to 27 µm represent 10 percent and particle size up to 80 µm represent 90%. Unexpectedly, the powder contains a large percentage of particles with the bigger diameter above 80 µm (Fig. 1).

3.2. Single track scans

To obtain basic information about SLM process the Single Track Scan (STS) test was performed (Fig. 2). The initial experiment consisted of forming single welds on a completely unused build platform. Laser power varied in the range of 100 W, 200 W, 300 W, 400 W and scanning speed in the range of 200 mm/s, 500 mm/s, 800 mm/s, 1100 mm/s and 1400 mm/s. Build platform was heated up to 80 °C. STS samples of 10 mm length were analyzed on the 3D optical profilometer (BrunkerContour GT X8).
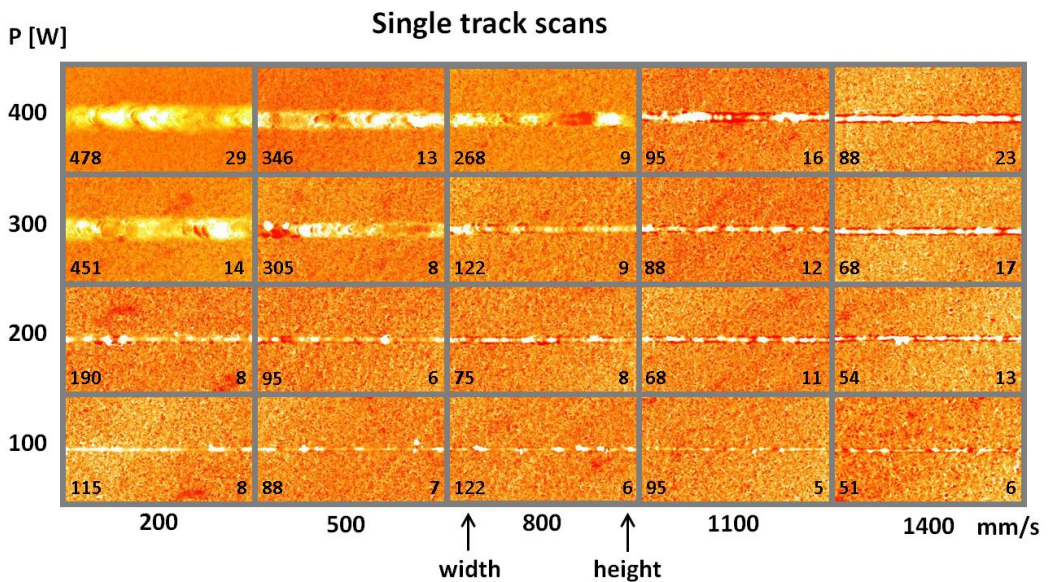

Fig. 2: Analysis of single track scans

Good welding characteristics is understood as a continuous weld and also smooth surface without balling effect. The best qualitative properties showed samples produced with laser power of 300 W and 400 W and a scanning speed of 1400 mm/s.

3.3. Thin wall test

The same range of laser power and laser speed was selected for thin wall test. The aim of the test is to identify the wall thickness depending on the laser power and the scanning speed. The same range of laser power and laser speed was selected for thin wall test. Walls with a surface energy density less than 2,86 J/mm2 were not involved in analysis because of insufficient welding integrity.

Thin walls were scanned using 3D optical scanner ATOS III Triple Scan 8M (GOM, Germany) with optical measuring volume MV60. The accuracy (0,003 mm) of scanner was evaluated according to "VDI/VDE 2634, Part 3: Optical 3D-measuring systems, multiple view systems based on area scanning" by vendor. Each wall was coated with thin titanium dioxide powder and methylated spirit to improve 3D digitizing conditions. Layer thickness of matte coating is approximately 0,002 mm.
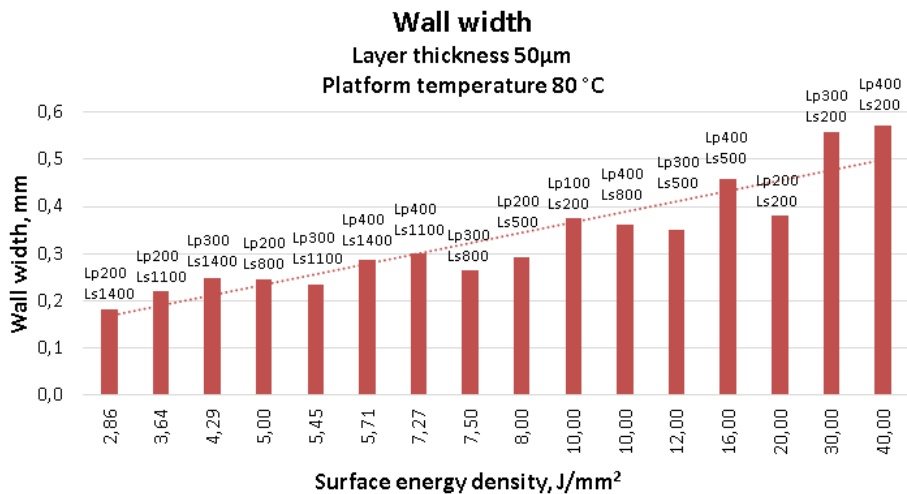

Fig. 3: Analyses of wall thickness

3.4. Cube samples

Single track scans and thin wall samples were initial test for preliminary selection of candidates for volumetric processing of the material (cube test). For full description of process parameters sixty four cubes (with 5mm edge) were built. All samples were built directly on reduction build plate. Three fundamental process parameters were selected to map the process window of 2618 alloy. Laser power (Lp) varied in range of 100, 200, 300, and 400W, laser scanning speed (Ls) varied in range of 200, 500, 800, 1100, 1400 mm/s. Values of hatch distance (Hd) were changed between 50 µm and 110 µm. The constant value 50 µm of layer thickness (Lt) was chosen. The scanning strategy was identical for all cube samples and it is shown on Figure 4. Parameters for the contour (red boarder lines) and the hatching (black arrows) were identical as well. Hatching angle changed over the height of the samples with increment of 90°.
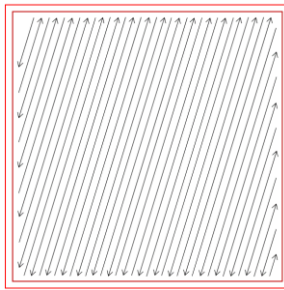
Fig. 4: Scanning strategy of all samples, stripe hatch

Totally 64 cube samples were manufactured in first stage. Samples were cut 1 mm from the top surface and initially evaluated just with digital camera (Fig. 5).
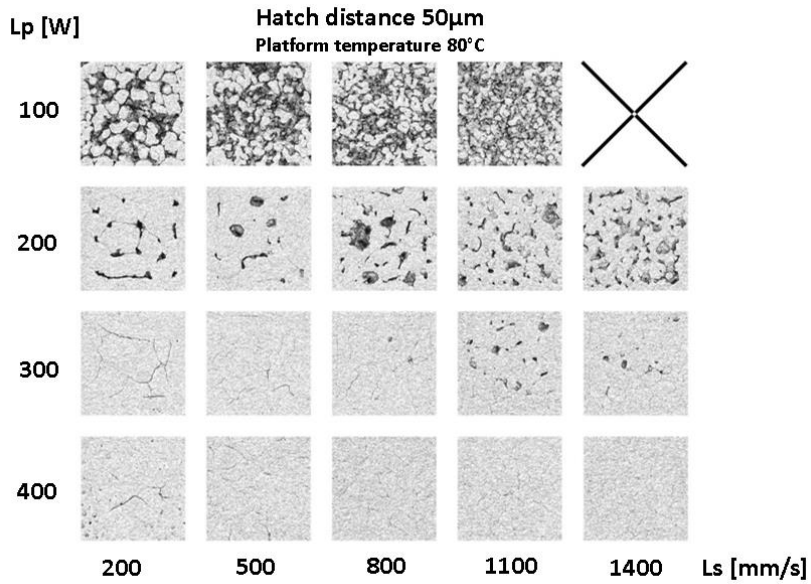

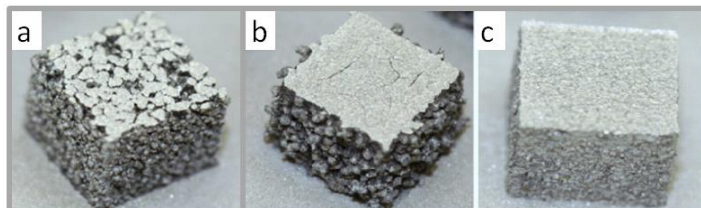Fig. 5: Preliminary analysis of the samples via camera with macro lens

Fig. 6: (a) Lp 100 W, Ls 200, Hd 110 μm, (b) Lp 300 W, Ls 200mm/s, Hd 50 μm, (c) Lp 400 W, Ls 1400mm/s, Hd 50 μm

3.5. Micro CT analysis of cube samples

After detachment and initial evaluation, the samples with laser power 100W were excluded from the further evaluation due to unsatisfactory consistence.

Group of eight cube samples were joined together into larger blocks. All blocks were analyzed by micro Computed Tomography (μCT) to determine the relative porosity and identify cracks and voids. The microCT analysis of the samples was performed using laboratory system GE phoenix v|tome|x M, equipped with a 300 kV/500W maximum power microfocus X-ray tube and high contrast flat panel detector DXR250 with 2048×2048 pixel, 200×200 μm pixel size. The exposure time was 250 ms in every of 2200 positions. The microCT scan was carried out at 130 kV and 100 μA acceleration voltage and X-ray tube current, respectively. The voxel size of obtained volumes was 12 μm. The tomographic reconstruction was realized using GE phoenix datos|x 2.0 3D computed tomography software.

Visualization of the sample and the porosity analysis were performed by the VG Studio MAX 2.2 software. The segmentation of pores was based on the simple thresholding procedure and the automatic tool of the VG Studio was used for the threshold determination. This tool determines the background peak and the material peak in the histogram and then calculates the gray value of the material boundary. The most of the micro cracks were not included to the pores analysis result because the cracks dimension is under the voxel resolution (meaning smaller than 12 μm). However the volume of those cracks does not significantly affect the total pores volume. Volume percentage of porosity ϕ was evaluated for each sample according the total volume of the pores and the bulk volume of the sample.
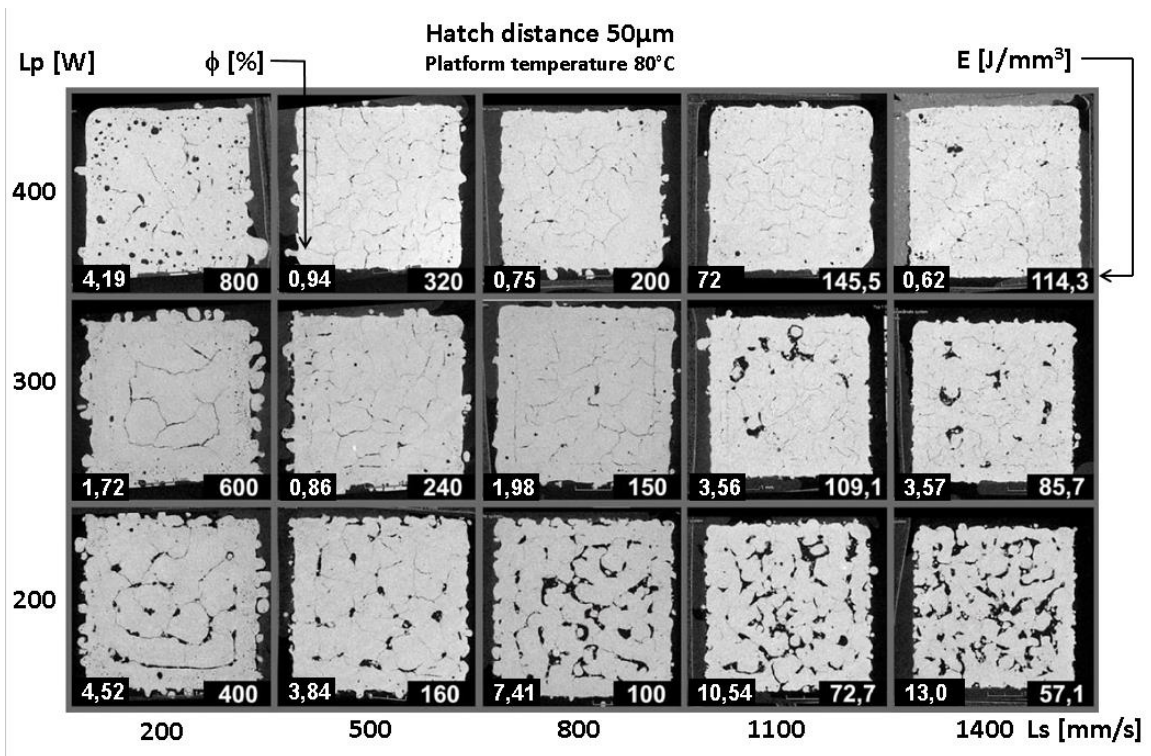

Fig. 7: μCT sections of samples, hatch distance 50μm

The results of µCT analysis (Fig. 7) show, that suitable process parameters areas regarding the porosity are those with higher laser power and higher laser speed. However, those samples also contain the high number of cracks visible even without metallurgical analysis. Therefore it is obvious, that the mechanical parameters of such samples would not reach those of conventional wrought material. It is expected, that the large amount of cracks in all samples is caused high temperature gradient and also high energy density E.

Energy density was calculated as:

$$E = \frac{Lp}{Ls \times Hd \times Lt} \; [\text{J/mm}^3]$$

(Lp) Laser power, (Ls) Scanning speed, (Hd) Hatch distance, (Lt) Layer thickness

Nevertheless several areas of interest were discovered. To eliminate cracks in the material additional series of sample cubes was evaluated (Fig. 8).
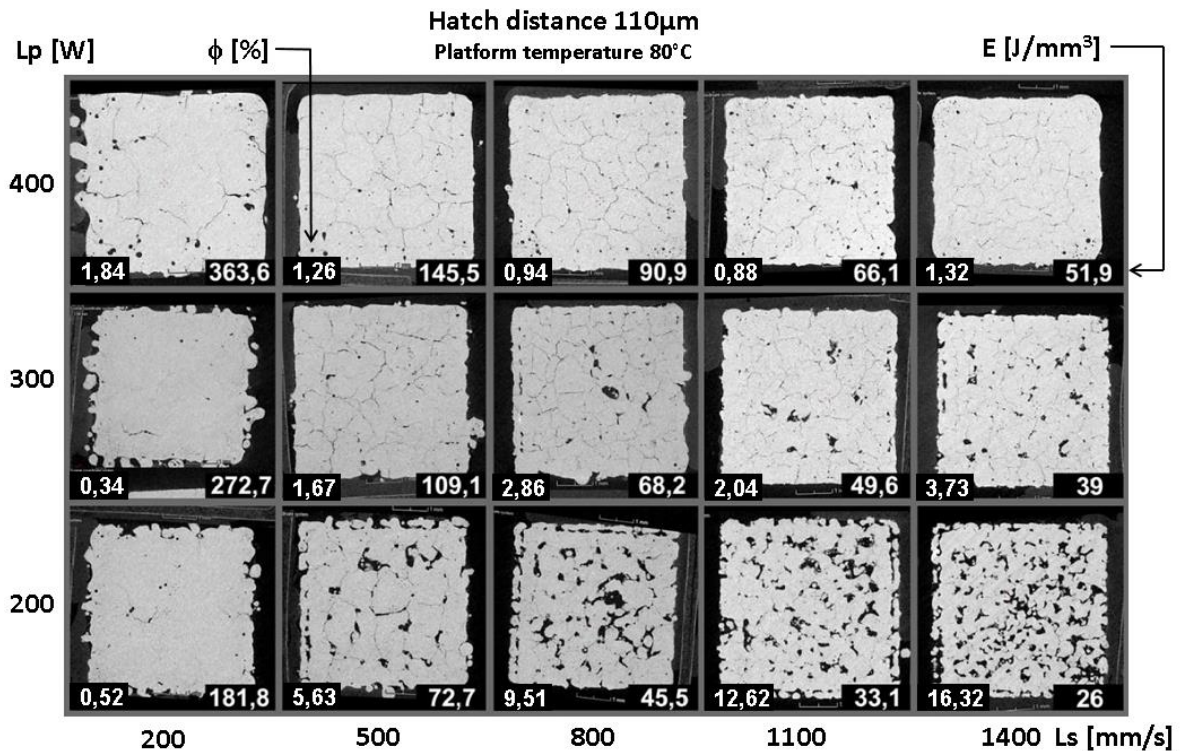

Fig. 8: µCT sections of samples, hatch distance 110µm

For the second test series hatch distance was set to value 110 µm. The energy of all variants is more than two times lower compared to hatch distance 50 µm. The µCT sections at Figure 8 show, similar results as first series of samples, however the sample with low laser power and low laser speed appears to be less susceptible to cracking. Relative density of samples was evaluated as well and the dependence of relative

density and scanning speed is shown on Fig. 9. For high laser power is the density more than 95 percent and seems to be independent on energy density. Lower laser power (200W) shows significant decrease in relative density with increasing laser speed (decreasing energy density).

Based on μCT analysis, two candidates according to the relative values of porosity and cracks occurrence were chosen as perspective. Samples with parameter 300W and 200W, laser speed 200 mm/s, hatch distance 110 μm show low volume of keyholes and cracks but energy is rather different. Both samples contain small cracks (Fig. 10). Better surface quality was achieved with laser power 400W and scanning speed 1400 mm/s.
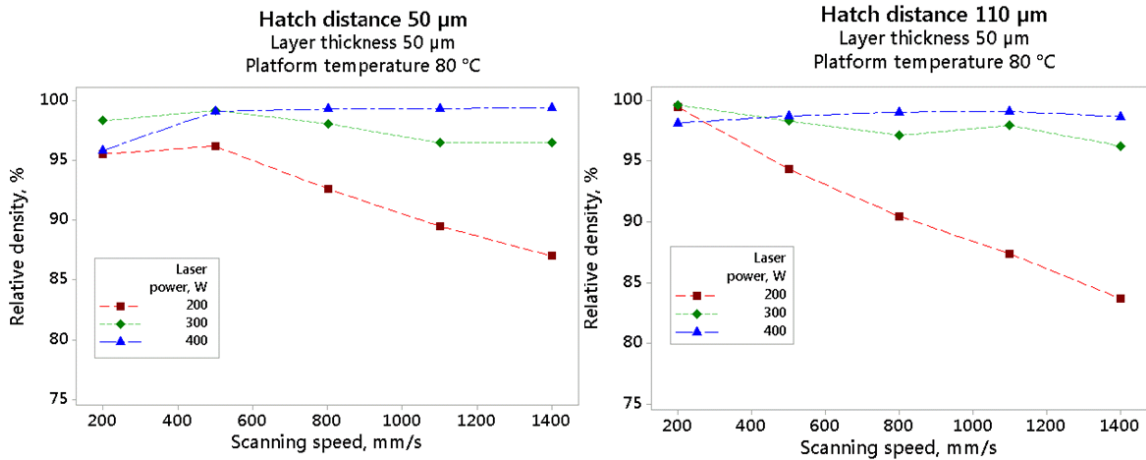

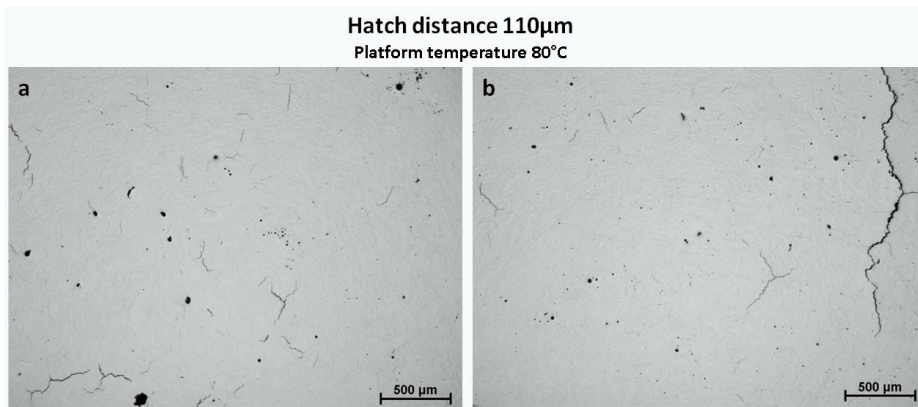Fig. 9: Dependence of relative density and scanning speed

Fig. 10: (a) Lp 200W, Ls 200mm/s, E=182 J/mm³, (b) Lp 300W, Ls 200mm/s, E=273 J/mm³ (light microscopy images)

4. Discussion

Relative porosity of samples was evaluated using μCT. Results show, that with the higher laser power (400W) a relative density higher than 99% can be reached, however with large amount of cracks. High propensity to cracking could be caused by high tempera gradient between the build plate and the solidifying melt pool, resulting in excessive cooling rate. However, heating of build plate to higher temperatures than

80°C was not possible due to use of reduction built plate. For further development of crack free material, the higher heating temperatures seems to be necessary.

Dependence of energy and relative density has not been proven, as was shown by Ahuja et al.. It seems that there is not a direct relationship between variables. Samples of the same value of volumetric energy density have a very different percentage of porosity. Such contradictory results could be caused by several influences, directly or indirectly affecting the production process. High energy input could influence whole process due to vaporization of particles, where the resulting splatter changes process conditions, mainly dissipation of laser beam. The quality of metal powder also affects the melting process. The powder of aluminum alloy 2618 contains many smaller particles which agglomerate into groups and adhering to larger particles. The particle size analysis of the used 2618 powder showed that 90% interval of the particle size is from 27 μm to 81 μm. Particles with unsuitable morphology or size can cause inhomogeneous powder layer, affects reflectivity, absorptivity and scattering of radiation.

Surface topology of samples depends on energy density. Lower surface roughness could be achieved with high laser power and scanning speed (400W and scanning speed 1400 mm/s.). Compared to that, high value of relative density was achieved with 200W of laser power and 200mm/s of laser speed (Fig. 6). The combination of high and low laser power at contour and volume areas respectively could produce high density parts with smoother surface.

5. Conclusion

Paper describe initial study of SLM process parameters of aluminium alloy 2618. The study provides an overview of the influence of main process parameters on porosity and macro-structure of the material. The main finding is that based on the energy density the porosity of samples cannot be considered. However, energy density affects process stability and surface roughness.

Some combination of process parameters result in material with relative density higher than 99%, which is promising, however such samples contain high amount of cracks, which would affect the mechanical behavior. Laser power 400 W and scan speed around 1400 mm/s and also low laser power below 200 W and slow scan speed 200 mm/s shows promising results and will be further studied.

References

Aboulkhair, Nesma T., Nicola M. Everitt, Ian Ashcroft, and Chris Tuck. 2014. "Reducing Porosity in AlSi10Mg Parts Processed by Selective Laser Melting." *Additive Manufacturing* 1-4. Elsevier B.V.: 77–86. doi:10.1016/j.addma.2014.08.001.
Ahuja, Bhrigu, Michael Karg, Konstantin Yu. Nagulin, and Michael Schmidt. 2014. "Fabrication and Characterization of High Strength Al-Cu Alloys Processed Using Laser Beam Melting in Metal Powder Bed." *Physics Procedia* 56. Elsevier B.V.: 135–46. doi:10.1016/j.phpro.2014.08.156.

Bartkowiak, Konrad, Sven Ullrich, Thomas Frick, and Michael Schmidt. 2011. "New Developments of Laser Processing Aluminium Alloys via Additive Manufacturing Technique." *Physics Procedia* 12 (January): 393–401. doi:10.1016/j.phpro.2011.03.050.

Brandl, Erhard, Ulrike Heckenberger, Vitus Holzinger, and Damien Buchbinder. 2012. "Additive Manufactured AlSi10Mg Samples Using Selective Laser Melting (SLM): Microstructure, High Cycle Fatigue, and Fracture Behavior." *Materials & Design* 34 (February). Elsevier Ltd: 159–69. doi:http://dx.doi.org/10.1016/j.matdes.2011.07.067.

Buchbinder, D., H. Schleifenbaum, S. Heidrich, W. Meiners, and J. Bültmann. 2011. "High Power Selective Laser Melting (HP SLM) of Aluminum Parts." *Physics Procedia* 12 (January): 271–78. doi:10.1016/j.phpro.2011.03.035.

Dadbakhsh, S., L. Hao, P.G.E. Jerrard, and D.Z. Zhang. 2012. "Experimental Investigation on Selective Laser Melting Behaviour and Processing Windows of in Situ Reacted Al/Fe2O3 Powder Mixture." *Powder Technology* 231 (November). Elsevier B.V.: 112–21. doi:10.1016/j.powtec.2012.07.061.

Dadbakhsh, Sasan, and Liang Hao. 2014. "Effect of Layer Thickness in Selective Laser Melting on Microstructure of Al/5 wt.%Fe2O3 Powder Consolidated Parts." *TheScientificWorldJournal* 2014 (January): 106129. doi:10.1155/2014/106129.

Fukuda, A, M Takemoto, T Saito, S Fujibayashi, M Neo, Deepak K Pattanayak, T Matsushita, et al. 2011. "Osteoinduction of Porous Ti Implants with a Channel Structure Fabricated by Selective Laser Melting." *Acta Biomaterialia* 7 (5): 2327–36. doi:10.1016/j.actbio.2011.01.037.

Jerrard P., Hao L., Dadbakhsh S., Evans K. 2011. "Consolidation Behaviour and Microstructural Characteristics of Al and a Mixture of Al-Cu Alloy Powders Following Selective Laser Melting Processing" 22: 371–81.

Kempen, K., L. Thijs, J. Van Humbeeck, and J.-P. P Kruth. 2012. "Mechanical Properties of AlSi10Mg Produced by Selective Laser Melting." *Physics Procedia* 39 (January): 439–46. doi:http://dx.doi.org/10.1016/j.phpro.2012.10.059.

Louvis, Eleftherios, Peter Fox, and Christopher J. Sutcliffe. 2011. "Selective Laser Melting of Aluminium Components." *Journal of Materials Processing Technology* 211 (2). Elsevier B.V.: 275–84. doi:10.1016/j.jmatprotec.2010.09.019.

Olakanmi, E.O. 2013. "Selective Laser Sintering/melting (SLS/SLM) of Pure Al, Al–Mg, and Al–Si Powders: Effect of Processing Conditions and Powder Properties." *Journal of Materials Processing Technology* 213 (8). Elsevier B.V.: 1387–1405. doi:10.1016/j.jmatprotec.2013.03.009.

Olakanmi, Eyitayo Olatunde, Kenneth W Dalgarno, and Robert F Cochrane. 2012. "Laser Sintering of Blended Al-Si Powders." *Rapid Prototyping Journal* 18 (2). Emerald: 109–19. doi:10.1108/13552541211212096.

Petters, Romy, Mihai Stoica, Sergio Scudino, Simon Pauly, and Lukas Lo. 2013. "Processing Metallic Glasses by Selective Laser Melting" 16 (February): 37–41.

Reinhart, Gunther, and Stefan Teufelhart. 2011. "Load-Adapted Design of Generative Manufactured Lattice Structures." *Physics Procedia* 12 (January): 385–92. doi:10.1016/j.phpro.2011.03.049.

Siddique, Shafaqat, Muhammad Imran, Eric Wycisk, Claus Emmelmann, and Frank Walther. 2015. "Influence of Process-Induced Microstructure and Imperfections on Mechanical Properties of AlSi12 Processed by Selective Laser Melting." *Journal of Materials Processing Technology* 221 (July): 205–13. doi:10.1016/j.jmatprotec.2015.02.023.

Thijs, Lore, Karolien Kempen, Jean-Pierre Kruth, and Jan Van Humbeeck. 2013. "Fine-Structured Aluminium Products with Controllable Texture by Selective Laser Melting of Pre-Alloyed AlSi10Mg Powder." *Acta Materialia* 61 (5): 1809–19. doi:10.1016/j.actamat.2012.11.052.

Weingarten, Christian, Damien Buchbinder, Norbert Pirch, Wilhelm Meiners, Konrad Wissenbach, and Reinhart Poprawe. 2015. "Formation and Reduction of Hydrogen Porosity during Selective Laser Melting of AlSi10Mg." *Journal of Materials Processing Technology* 221 (July): 112–20. doi:10.1016/j.jmatprotec.2015.02.013.

Wohlers, T T. 2014. *Wohlers Report 2014: 3D Printing and Additive Manufacturing State of the Industry Annual Worldwide Progress Report*. Wohlers Associates. https://books.google.cz/books?id=iCamoAEACAAJ.

Wong, M., I. Owen, C.J. Sutcliffe, and A. Puri. 2009. "Convective Heat Transfer and Pressure Losses across Novel Heat Sinks Fabricated by Selective Laser Melting." *International Journal of Heat and Mass Transfer* 52 (1-2): 281–88. doi:10.1016/j.ijheatmasstransfer.2008.06.002.